Talanta 85 (2011) 1627–1633

Contents lists available at ScienceDirect

Talanta

journal homepage: www.elsevier.com/locate/talanta

"Off-On" based fluorescent chemosensor for Cu^{2+} in aqueous media and living cells

Chunwei Yu[a,d], Lingxin Chen[a,*], Jun Zhang[c], Jinhua Li[a], Ping Liu[a], Wenhai Wang[a], Bing Yan[b,**]

[a] Key Laboratory of Coastal Zone Environmental Processes, CAS, Shandong Provincial Key Laboratory of Coastal Zone Environmental Processes, Yantai Institute of Coastal Zone Research, Chinese Academy of Sciences, Yantai 264003, China
[b] School of Chemistry and Chemical Engineering, Shandong University, Jinan 250100, China
[c] School of Tropical and Laboratory Medicine, Hainan Medical University, Haikou 571101, China
[d] Graduate University of Chinese Academy of Sciences, Beijing 100049, China

ARTICLE INFO

Article history:
Received 8 April 2011
Received in revised form 18 June 2011
Accepted 22 June 2011
Available online 29 June 2011

Keywords:
Cu^{2+}
Fluorescent chemosensor
Rhodamine B
Fluorescence imaging
Living cells

ABSTRACT

A novel Cu^{2+}-specific "off-on" fluorescent chemosensor of naphthalimide modified rhodamine B (*n*aphthalimide modified *r*hodamine B *c*hemosensor, **NRC**) was designed and synthesized, based on the equilibrium between the spirolactam (non-fluorescence) and the ring-opened amide (fluorescence). The chemosensor **NRC** showed high Cu^{2+}-selective fluorescence enhancement over commonly coexistent metal ions or anions in neutral aqueous media. The limit of detection (LOD) based on $3 \times \delta_{blank}/k$ was obtained as low as 0.18 μM of Cu^{2+}, as well as an excellent linearity of 0.05–4.5 μM ($R = 0.999$), indicating the chemosensor of high sensitivity and wide quantitation range. And also the coordination mode with 1:1 stoichiometry was proposed between **NRC** and Cu^{2+}. In addition, the effects of pH, co-existing metal ions and anions, and the reversibility were investigated in detail. It was also demonstrated that the **NRC** could be used as an excellent "off-on" fluorescent chemosensor for the measurement of Cu^{2+} in living cells with satisfying results, which further displayed its valuable applications in biological systems.

1. Introduction

Chemosensors that convert molecular recognition into highly sensitive, quick and nondestructive fluorescent signals have been actively investigated [1]. Among them, sensing of Cu^{2+} has received ever-increasing attention, since Cu^{2+} plays a critical role as a catalytic co-factor for a variety of metalloenzymes, including superoxide dismutase, cytochrome *c* oxidase, tyrosinase and so on [2]. However, under overloading conditions, Cu^{2+} can cause oxidative stress and disorders associated with neurodegenerative diseases, such as Alzheimer's disease, Wilson's disease, and Menke's disease, probably by its involvement in the production of reactive oxygen species [3]. Thus far, fluorescent probes for copper ion have been extensively explored owing to its biological significance. Even though great achievements have been obtained in the field of colorimetric and/or fluorescent chemosensors for Cu^{2+} [4], most of the reported Cu^{2+} fluorescent chemosensors cause a quenching of the fluorescence emission upon addition of this metal ion due to its paramagnetic nature [5,6]. Only a few chemosensors in which the binding of Cu^{2+} leads to an increase in the fluorescence intensity have been found, which are desirable for analytical purposes by the fluorescence enhancement [7]. However, those chemosensors are still rarely applied in neutral aqueous systems due to the strong hydration ability of Cu^{2+} in aqueous solution. And most of them only work well in strong acidic solution. Moreover, most of these fluorescent chemosensors are excited by UV light. These limitations lower the sensitivity and restrict their applications in environmental and biological samples. Therefore, it is of importance to develop some rapid and "simple-to-use" fluorescent chemosensors with Cu^{2+} induced "turn-on" fluorescence signal, in neutral aqueous buffer containing less than 20% organic cosolvent or in neutral pure water.

Fluorescence imaging technology was regarded as an advanced method for visualizing distribution of Cu^{2+} in physiological process by virtue of its excellent properties [8]. Development of highly sensitive, selective, and cell membrane-penetrable chemosensors that exhibit a visible fluorescence enhancement in aqueous media is an eternal theme of innovation for the measurement of metal ions in living cells. In recent years, several fluorescence "off-on" chemosensors for imaging various intracellular metal ions have been introduced successively [9]. However, few of chemosensors have been reported for imaging Cu^{2+} in living cells. Salicylaldehyde substructure-based compounds are known as a molecular platform for the construction of chemosensors for Cu^{2+} [7e,10,11]. On the other hand, rhodamine derivatives are non-fluorescent and

* Corresponding author.
** Corresponding author.
E-mail addresses: lxchen@yic.ac.cn (L. Chen), dr.bingyan@gmail.com (B. Yan).

0039-9140/$ – see front matter © 2011 Elsevier B.V. All rights reserved.
doi:10.1016/j.talanta.2011.06.057

colorless, whereas ring-opening of the corresponding spirolactam gives rise to strong fluorescence emission and a pink color, the progress has been fully utilized for the detection of metal ions and H^+ [12].

Herein, a novel "off-on" based fluorescent chemosensor composed of naphthalimide modified rhodamine B derivative (*n*aphthalimide modified *r*hodamine B *c*hemosensor, **NRC**) was successfully designed and synthesized, for high selective and sensitive determination of Cu^{2+} in aqueous media and living cells. The effects of pH, co-existing metal ions and anions, and the reversibility of **NRC** were systematically investigated. For comparison, compound ***p*-NRC** was synthesized to test the optical change for Cu^{2+}. And also the possible sensing mechanism was proposed. The developed chemosensor was displayed promising for rapid and sensitive determination of Cu^{2+} in vitro in biological samples, even potentially in vivo monitoring.

2. Experimental

2.1. Apparatus

NMR spectra were collected in $CDCl_3$ or DMSO-d_6 at 25 °C on a Bruker WM-300 spectrometer (Germany). Electrospray ionization (ESI) analyses were performed on a Thermo TSQ Quantum Mass Spectrometer (Germany), method parameters: Sheath Gas Flow Rate (arb): 30; Aux Gas Flow Rate (arb): 10; Capillary Temp. (°C): 300; Capillary Voltage (V): −45.00 (ES−)/10.00 (ES+); Spray Voltage (kV): 5.00. UV–vis spectra were obtained on a Beckman DU-800 spectrophotometer (USA) with 1 cm quartz cell at 25 °C. Fluorescence measurements were carried out on a Perkin Elmer LS55 luminescence spectrometer (USA). Fluorescence imaging was performed by confocal fluorescence microscopy on an Olympus FluoView Fv1000 laser scanning microscope (USA). Melting points were determined using a Shanghai Melting points WRS-1B apparatus (Shanghai, China). pH values were measured with a pH-meter PBS-3C (Shanghai, China).

2.2. Materials

All reagents and solvents are of analytical grade and used without further purification, which are all purchased from Sinopharm Chemical Reagent Co. Ltd. (China). Cation species employed were from NaCl, $MgCl_2{\cdot}6H_2O$, $CdCl_2$, $HgCl_2$, $CaCl_2{\cdot}2H_2O$, $FeCl_3{\cdot}6H_2O$, $CrCl_3{\cdot}6H_2O$, $Zn(NO_3)_2{\cdot}6H_2O$, $AgNO_3$, $CoCl_2{\cdot}6H_2O$, $MnCl_2{\cdot}4H_2O$, $CuCl_2{\cdot}2H_2O$, $NiCl_2{\cdot}6H_2O$, and $PbCl_2$, respectively. Anion species from various salts such as NaClO, $NaNO_3$, Na_2CO_3, NaCl, NaAc, $NaClO_4$, KBr and Na_2HPO_4. Cations and anions were dissolved in deionized water and chemosensor was dissolved in tetrahydrofuran (THF) to obtain 1 mM stock solutions, respectively.

2.3. Synthesis of compounds

Compound **3** and compound **6** were synthesized following the reported literatures [13,14]. Compounds **4**, **5**, **NRC** and ***p*-NRC** were characterized by ^{1}H NMR, ^{13}C NMR, elementary analysis and ESI-MS (Fig. S9–S20 in Supporting Information). Synthesis routes of compounds **NRC** and ***p*-NRC** are provided in Scheme 1, and corresponding synthesis details are as follows. And then, the obtained **NRC** and ***p*-NRC** were dissolved in THF to obtain 1 mM stock solutions for use, respectively. That needs explanation is, for clarity, the synthesized compounds are described using serial number instead of special names as reported [11].

2.3.1. Compound *4*

Under N_2 gas, compound **3** (300 mg, 0.90 mmol) and K_2CO_3 (500 mg, 3.62 mmol) were combined in DMF (10 mL) and stirred. 2,4-Dihydroxybenzaldehyde (130 mg, 0.9 mmol) in DMF (10 mL) was added dropwise. The reaction mixture was stirred at 80 °C for 12 h, filtered through celite and the solvent was evaporated under reduced pressure, purification with silica gel column chromatography (CH_2Cl_2/petroleum ether = 15:1, v:v) afforded as a yellow solid. Yields: 245 mg (70%). ^{1}H NMR (δ: ppm, $CDCl_3$): 11.37 (s, 1H, CHO), 9.85 (s, 1H, OH), 8.65–8.67 (d, 1H, ArH), 8.56–8.57 (d, 1H, ArH), 8.44–8.46 (d, 1H, ArH), 7.76–7.79 (t, 1H, ArH), 7.59–7.61 (d, 1H, ArH), 7.26–7.27 (t, 1H, ArH), 6.73–6.76 (d, 1H, ArH), 6.61–6.62 (d, 1H, ArH), 4.18–4.21 (t, 2H, $-NCH_2$), 1.70–1.76 (m, 2H, CH_2), 1.42–1.49 (m, 2H, CH_2), 0.97–1.00 (t, 3H, CH_3). ^{13}C NMR (δ: ppm, $CDCl_3$): 194.94 (CHO), 164.08, 163.48 (C=O), 156.48, 136.03, 132.55, 132.25, 132.05, 131.03, 129.81, 128.08, 127.19, 124.74, 123.03, 119.12, 117.62, 115.10, 110.73, 106.80, 40.30, 30.23, 20.39, 13.85. MS (ES−) m/z: 388.11 $[M-H]^-$. Anal. Calcd. for $C_{23}H_{19}NO_5$ (389.40): C, 70.94; H, 4.92; N, 3.60. Found: C, 70.26; H, 5.36; N, 3.54.

2.3.2. Compound *5*

Under N_2 gas, compound **3** (500 mg, 1.5 mmol) and K_2CO_3 (900 mg, 6.52 mmol) were combined in DMF (50 mL) and stirred. 4-Hydroxy benzaldehyde (220 mg, 1.8 mmol) in DMF (10 mL) was added dropwise. The reaction mixture was stirred at 80 °C for 12 h. The mixture was cooled and poured into ice-water. The precipitate produced was filtered and further purified by recrystallization from ethanol. Yields: 448 mg (80%). ^{1}H NMR (δ: ppm, $CDCl_3$): 10.03 (s, 1H, CHO), 8.67–8.69 (d, 1H, ArH), 8.53–8.57 (m, 2H, ArH), 8.00 (t, 1H, ArH), 7.98–7.99 (t, 1H, ArH), 7.78–7.81 (m, 1H, ArH), 7.29–7.30 (t, 1H, ArH), 7.28 (s, 1H, ArH), 7.14–7.16 (d, 1H, ArH), 4.18–4.22 (t, 2H, $-NCH_2$), 1.71–1.77 (m, 2H, CH_2), 1.43–1.51 (m, 2H, CH_2), 0.98–1.01 (t, 3H, CH_3). ^{13}C NMR (δ: ppm, $CDCl_3$): 190.50 (CHO), 164.12, 163.52 (C=O), 160.89, 157.54, 133.12, 132.36, 132.23, 132.05, 129.80, 128.15, 127.05, 124.48, 122.96, 119.77, 118.47, 113.50, 40.27, 30.24, 20.39, 13.85. MS (ES+) m/z: 374.13 $[M+H]^+$. Anal. Calcd. for $C_{23}H_{19}NO_4$ (373.40): C, 73.98; H, 5.13; N, 3.75. Found: C, 74.07; H, 5.66; N, 3.66.

2.3.3. Compound *NRC*

A stirred solution of compound **6** (176 mg, 0.39 mmol) and compound **4** (150 mg, 0.39 mmol) in ethanol (30 mL) was heated to reflux for 12 h under N_2 gas. The precipitate produced was filtered and washed with hot ethanol (5 mL × 3). After drying under reduced pressure, a yellow solid was obtained. Yields: 248 mg (75%). M.p.: 258.6–259.1 °C. ^{1}H NMR (δ: ppm, $CDCl_3$): 11.15 (s, 1H, OH), 9.33 (s, 1H, ArH), 8.62–8.64 (d, 1H, ArH), 8.54–8.54 (d, 1H, ArH), 8.44–8.46 (d, 1H, ArH), 7.98–7.99 (d, 1H, ArH), 7.71–7.74 (t, 1H, ArH), 7.52–7.58 (m, 1H, ArH), 7.19–7.20 (d, 1H, ArH), 7.16–7.19 (d, 1H, ArH), 7.01–7.02 (d, 1H, ArH), 6.60–6.61 (d, 1H, ArH), 6.56–6.59 (d, 1H, ArH), 6.51 (s, 1H, ArH), 6.49 (s, 1H, ArH), 6.47 (d, 2H, ArH), 6.29–6.30 (d, 1H, ArH), 6.27–6.28 (d, 1H, ArH), 4.16–4.19 (t, 2H, $-CH_2$), 3.31–3.35 (m, 8H, ArH), 1.68–1.74 (m, 2H, ArH), 1.41–1.18 (m, 2H, ArH), 1.14–1.17 (t, 12H, $-CH_3$), 0.96–0.99 (t, 3H, $-CH_3$). ^{13}C NMR (δ: ppm, $CDCl_3$): 164.33, 164.26, 163.70 (C=O), 160.65, 158.53, 157.76, 153.67, 152.21, 150.53, 149.12, 133.55, 133.07, 132.57, 131.84, 130.14, 129.69, 128.67, 128.47, 128.16, 126.62, 124.26, 123.33, 122.74, 117.44, 116.15, 112.47, 110.66, 108.32, 108.14, 105.41, 97.98 (Ar–C), 66.63, 44.36, 40.19, 30.25, 20.40, 13.86, 12.61. MS (ES−) m/z: 826.30 $[M-H]^-$. Anal. Calcd. for $C_{51}H_{49}N_5O_6$ (827.96): C, 73.98; H, 5.97; N, 8.46. Found: C, 74.22; H, 5.77; N, 8.38.

2.3.4. Compound *p-NRC*

Compound ***p*-NRC** was synthesized following the similar procedure of compound **NRC** by the reaction of compound **6** with compound **5**. ^{1}H NMR (δ: ppm, $CDCl_3$): 8.76 (s, 1H, ArH), 8.56–8.57 (d, 1H, ArH), 8.53–8.55 (d, 1H, ArH), 8.34–8.36 (d, 1H, ArH), 7.92–7.93 (d, 1H, ArH), 7.66–7.69 (t, 1H, ArH), 7.58 (s, 1H, ArH),

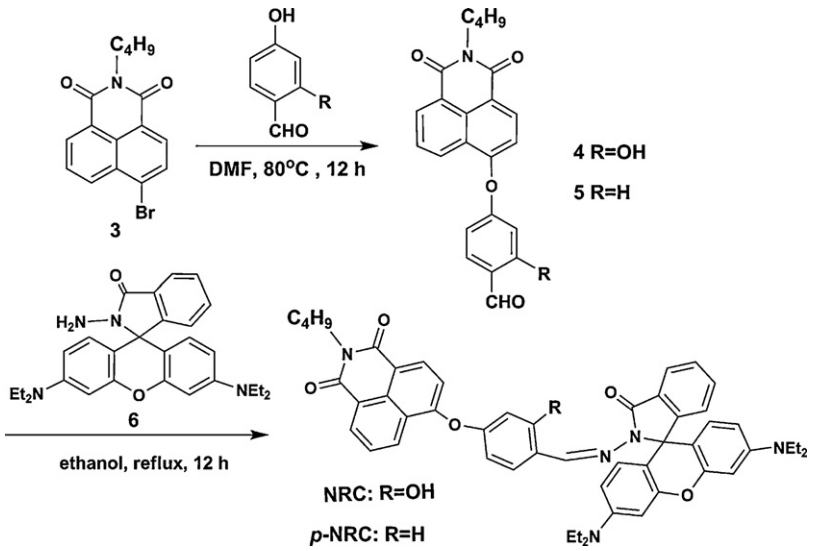

Scheme 1. Chemical structure and synthesis route of naphthalimide modified rhodamine B-based fluorescent chemosensor **NRC**.

7.56 (s, 1H, ArH), 7.39–7.46 (m, 2H, ArH), 7.06–7.08 (d, 1H, ArH), 6.98–7.00 (d, 2H, ArH), 6.82–6.83 (d, 1H, ArH), 6.45–6.47 (d, 2H, ArH), 6.37–6.38 (d, 2H, ArH), 6.20–6.21 (d, 1H, ArH), 6.18–6.19 (d, 1H, ArH), 4.08–4.11 (t, 2H, $-NCH_2CH_2-$), 3.24–3.28 (m, 8H, NCH_2), 1.60–1.67 (m, 2H, CH_2), 1.33–1.41 (m, 2H, CH_2), 1.07–1.10 (t, 12H, CH_3), 0.89–0.92 (t, 3H, CH_3). ^{13}C NMR (δ: ppm, $CDCl_3$): 164.95, 164.36, 163.72 (C=O), 159.27, 156.10, 153.29, 151.56, 148.95, 146.22, 133.40, 132.94, 132.65, 131.87, 129.69, 129.52, 129.48, 128.46, 128.37, 128.08, 126.57, 124.02, 123.96, 123.38, 122.72, 120.31, 117.04, 111.30, 108.02, 106.20, 97.91 (Ar–C), 66.19, 58.48, 44.34, 40.18, 30.25, 20.48, 18.45, 13.86, 12.62. MS (ES+) m/z: 812.30 $[M+H]^+$. Anal. Calcd. for $C_{51}H_{49}N_5O_5$ (811.37): C, 75.44; H, 6.08; N, 8.63. Found: C, 75.29; H, 6.48; N, 8.38.

2.4. UV–vis and fluorescence titration

Test solutions were prepared by placing 50 μL of the **NRC** stock solution (1 mM) into a test tube, adding an appropriate aliquot of individual ions stock solution (1 mM), and then diluting the solution to 5 mL with ethanol/HEPES (1:9, v:v, 50 mM, pH 7.0). For pH effect study, a series of HEPES buffers (50 mM) were prepared with different pH values adjusted by adding certain amounts of 1 M HCl or 1 M NaOH. All of the UV–vis and fluorescence titration data were recorded at room temperature.

2.5. Cell incubation and imaging

HeLa cells placed on coverslips were washed with phosphate-buffered saline (PBS), followed by incubating with 1 μM of $CuCl_2$ (in PBS) for 30 min at 37 °C, and then washed with PBS three times. After incubating with 20 μM of chemosensor **NRC** for 30 min at 37 °C, and then the cells were washed with PBS three times again. Fluorescence imaging of intracellular Cu^{2+} in HeLa cells was conducted by using a confocal fluorescence microscopy on an Olympus FluoView Fv1000 laser scanning microscope.

3. Results and discussion

3.1. Effects of pH on *NRC* and *NRC* with Cu^{2+}

The pH-control emission measurements revealed that the chemosensor **NRC** could respond to Cu^{2+} and showed less than 10% change in the pH range of 4.8–9.2 with the fluorescent intensity varying, while the fluorescence from the free **NRC** could be negligible, as seen from Fig. 1. It can be concluded that the **NRC** facilitates the concentration quantification of Cu^{2+} in a wide pH range. And this also suggests the chemosensor **NRC** is potentially applicable to the sensing for Cu^{2+} in aqueous and/or biological media.

3.2. Colorimetric and fluorescent signaling of Cu^{2+}

To gain more insight into the chemosensing properties and mechanism of **NRC** toward Cu^{2+}, absorption titration (Fig. 2) and fluorescence titration (Fig. 3) with Cu^{2+} were recorded, respectively. As seen from Fig. 2, upon sequential addition of Cu^{2+}, the absorption band centered at 391 and 556 nm appeared with increasing intensity, which induced a clear color change from pale yellow to pink; meanwhile, the band at 330 nm decreased gradually in intensity, with two isosbestic points at 315 and 356 nm. A linear dependence of absorbance at 556 nm was observed as a function of Cu^{2+} concentration (inset of Fig. 2), and thereby the stoichiometry of **NRC** with Cu^{2+} could be estimated to be 1:1. Moreover, the Job's plot (Fig. S1 in Supporting Information) clearly confirmed the 1:1 stoichiometry for **NRC**–Cu^{2+} complex, which was also supported by

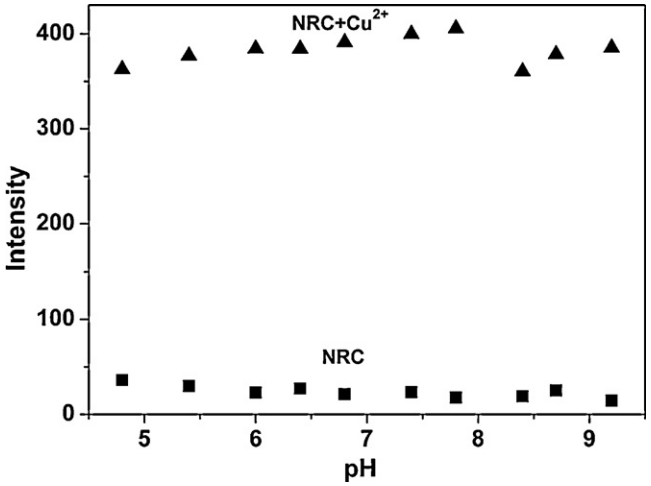

Fig. 1. Influences of pH on the fluorescence spectra of NRC (5 μM) (■) and NRC (5 μM) plus Cu^{2+} (50 μM) (▲) in ethanol–water solution (1:9, v:v). The pH was modulated by adding 1 M HCl or 1 M NaOH in HEPES buffers.

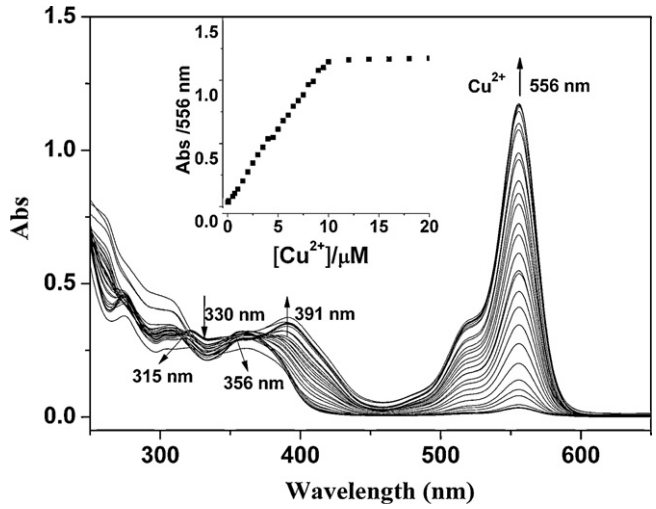

Fig. 2. Absorbance spectra of **NRC** (10 μM) in ethanol–water solution (1:9, v:v, 50 mM HEPES, pH 7.0) in the presence of different amounts of Cu^{2+}. Inset: absorption at 556 nm as a function of Cu^{2+} concentration.

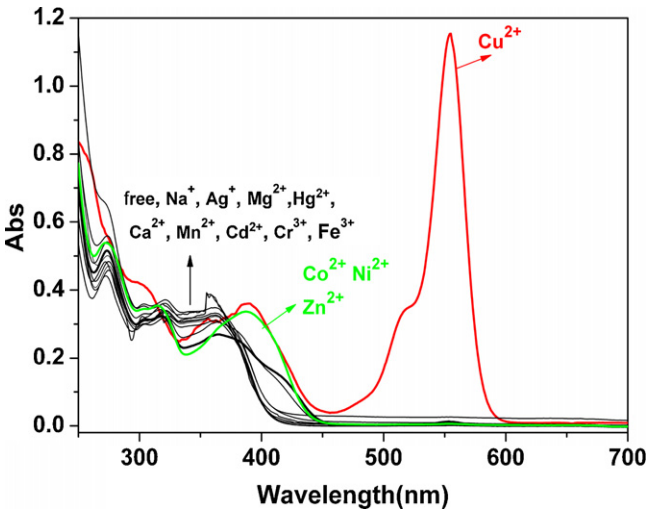

Fig. 4. UV–vis spectra of **NRC** (10 μM) with different metal ions (10 equiv.) in ethanol–water solution (1:9, v:v, 50 mM HEPES, pH 7.0).

ESI-MS (Fig. S2 in Supporting Information), where a main peak at 889.32 (*m/z*) corresponded to [**NRC** + Cu^{2+}–H]$^+$.

As seen from Fig. 3, upon the gradual addition of Cu^{2+}, an emission band peaked at 580 nm significantly increased in fluorescence intensity, possibly because of the rhodamine ring-opening process [11,12], which allowed a direct fluorescence detection of Cu^{2+}. On the basis of 1:1 stoichiometric relationship mentioned above, the linear fluorescence enhancement of **NRC** (5 μM) toward amounts of Cu^{2+} added was obtained in the range of 0.05–4.5 μM (R = 0.999) (inset of Fig. 3). The limit of detection (LOD) was attained of 0.018 μM, based on $3 \times \delta_{blank}/k$ (where δ_{blank} is the standard deviation of the blank solution and k is the slope of the calibration plot). The results indicated that the **NRC** chemosensor could sensitively detect environmentally relevant levels of Cu^{2+}.

To further investigate the selectivity of the fluorescent chemosensor, fluorescence measurements were also carried out toward various metal ions, by using the excitation wavelength 360 nm of naphthalimide fluorophore. As expected, **NRC** exhibited excellent selectivity for Cu^{2+} over alkali and alkaline-earth metal ions (Fig. S3 in Supporting Information). These facts indicated that NRC was induced to form the open-ring structure by Cu^{2+} from the spirolactam form [11,12].

Additionally, for different amounts of Cu^{2+}, the intensity of the fluorescent peak at 450 nm gradually decreased and that of a new fluorescent band centered at 580 nm gradually increased (Fig. S4 in Supporting Information). This observation is consistent with increased fluorescence resonance energy transfer (FRET) from 1,8-naphthalimide (donor) to the open, colored form of rhodamine (acceptor) (Scheme 2). However, the efficient FRET was observed only upon addition of 10 equiv. Cu^{2+} to the solution of NRC (5 μM) (Fig. S4 in Supporting Information), since there is a weak spectral overlap between 1,8-naphthalimide emission and rhodamine absorption.

3.3. Possible sensing mechanism

The mechanism for these optical changes was investigated. For comparison, compound ***p*-NRC** was also synthesized. As seen from Fig. S5 (in Supporting Information), the UV–vis absorption spectra of ***p*-NRC** to various other metal ions, neither the color nor the absorption spectra varied, as well as to Cu^{2+}; whereas upon addition of Cu^{2+} to a yellow solution of **NRC**, fluorescent and colorimetric characteristics of rhodamine B appeared (Figs. 4 and 5).

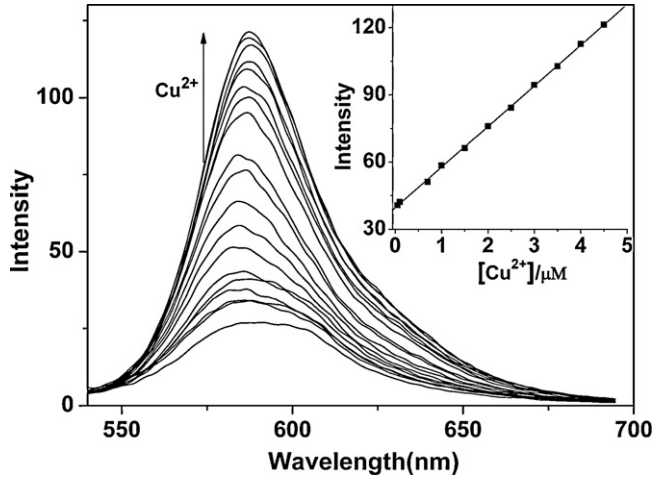

Fig. 3. Fluorescence spectra of **NRC** (5 μM) in ethanol–water solution (1:9, v:v, 50 mM HEPES, pH 7.0) in the presence of different amounts of Cu^{2+}. Inset: the fluorescence intensity at 580 nm as a function of Cu^{2+} concentration. Excitation wavelength was 510 nm.

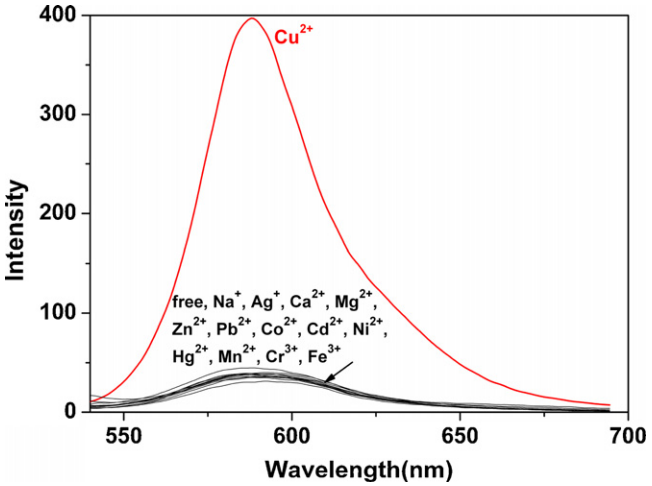

Fig. 5. Fluorescence spectra of **NRC** (5 μM) with different metal ions (10 equiv.) in ethanol-water solution (1:9, v:v, 50 mM HEPES, pH 7.0).

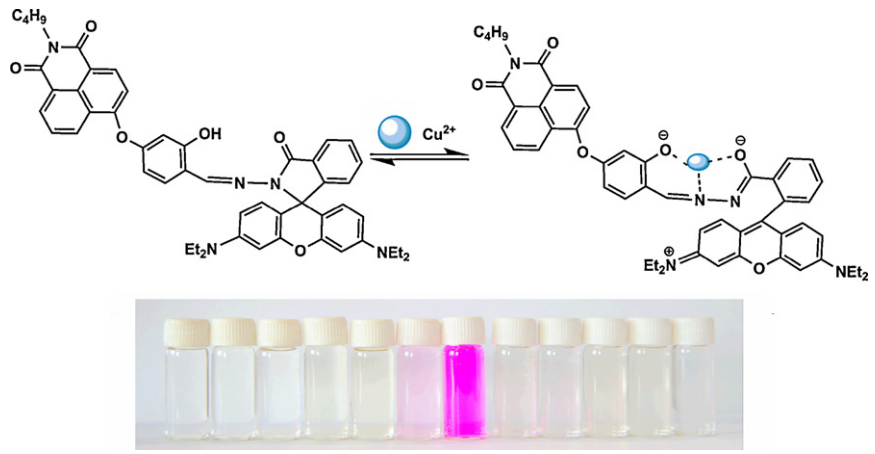

Scheme 2. Binding mode of **NRC** with Cu^{2+}. Bottom: photograph of **NRC** (10 μM) as a selective naked-eye chemosensor for Cu^{2+} in ethanol–water solution (v/v, 1:9, 50 mM HEPES, pH 7.0), upon addition of 100 μM individual metal ion including Na^+, Ag^+, Mg^{2+}, Zn^{2+}, Pb^{2+}, Fe^{3+}, Cu^{2+}, Mn^{2+}, Cd^{2+}, Ni^{2+}, Co^{2+}, and Hg^{2+} (from left to right).

This indicated that the hydroxy group in coupound **NRC** indeed played an important role in the course of binding with Cu^{2+}. And these changes can be attributed to the structure transformation from spirolactam (non-fluorescence) to ring-opened amide (fluorescence) [12], due to the complexation of Cu^{2+}. Moreover, the binding constant of $4.2 \times 10^5\ M^{-1}$ was obtained according to the Benesi–Hildebrand method [15], which suggested the strong interaction of **NRC** with Cu^{2+}. Thus, the desirable appearance and enhancement of fluorescence enables the favorable sensing for Cu^{2+}.

The proposed binding mode of **NRC** with Cu^{2+} is illustrated in Scheme 2, namely oxygen on the naphthalimide, oxygen on the carbonyl group, as well as nitrogen on the hydrazine moiety can cooperatively coordinate with Cu^{2+}. It is believed that this process is reversible, which has been proved by the test using EDTA-Cu^{2+} (Figs. S6 and S7 in Supporting Information). As seen, without Cu^{2+}, chemosensor **NRC** existed in a non-fluorescence spirocyclic form. Addition of Cu^{2+} led to reversible coordination with the ligand groups, resulting in spiro-cycle opening along with an appearance of orange fluorescence and a clear color change from colorless to pink (Bottom of Scheme 2). Thus, an "off-on" based fluorescent chemosensor for Cu^{2+} was constructed.

3.4. Interference studies from other metal ions and anions

The UV–vis and fluorescence responses of **NRC** to various possible interfering metal ions and anions and its selectivity for Cu^{2+} were tested. Shown in Fig. 4, only the Cu^{2+} induced a notable color change in buffer solution, which can be ascribed to the spirolactam bond cleavage of rhodamine group [12], while the other cations did not give rise to any obvious absorbance response. Addition of Na^+, Ag^+, Zn^{2+}, Pb^{2+}, Co^{2+}, Cd^{2+}, Ni^{2+}, Ca^{2+}, Mg^{2+}, Hg^{2+}, Cr^{3+} and Fe^{3+} exerted little or no effect on the emission of **NRC**, while remarkable fluorescence enhancement was detected upon the addition of Cu^{2+} by excitation of the rhodamine fluorophore at 510 nm, shown in Fig. 5. Furthermore, in the competition experiments, the fluorescence properties of **NRC** toward other metal ions (above-mentioned) were measured, showing that the increase of fluorescence intensity resulting from the addition of the Cu^{2+} was not influenced by the addition of excess metal ions (Fig. S8(a) in Supporting Information). Also, it was investigated that the fluorescence response of chemosensor **NRC** toward Cu^{2+} in the presence of various commonly coexistent anions such as ClO^-, NO_3^-, CO_3^{2-}, Cl^-, Ac^-, ClO_4^-, Br^- and HPO_4^{2-}. It is gratifying to note that all the tested anions have no obvious influence on the chemosensor **NRC** function (Fig. S8(b) in Supporting Information). All of these findings indicated that **NRC** was a highly selective colorimetric and fluorescent chemosensor for Cu^{2+} in aqueous buffer solution.

3.5. Fluorescence imaging of living cells for Cu^{2+}

To further demonstrate the practical applicability of the chemosensor **NRC** for Cu^{2+} in biological samples, fluorescence imaging was performed in living cells, since the **NRC** has been proved applicable to neutral aqueous media. HeLa cells were chosen and their fluorescence images were recorded before and after the addition of Cu^{2+} (Fig. 6) by using the excitation wavelength at 559 nm. For the cells treated with 20 μM **NRC** alone for 30 min at 37 °C, no obvious fluorescence was found (Fig. 6(a)). Excitedly, under the same conditions, the significant fluorescence enhancement was observed (Fig. 6(c)), when the cells were incubated with 1 μM $CuCl_2$ in the growth medium for 30 min at 37 °C and

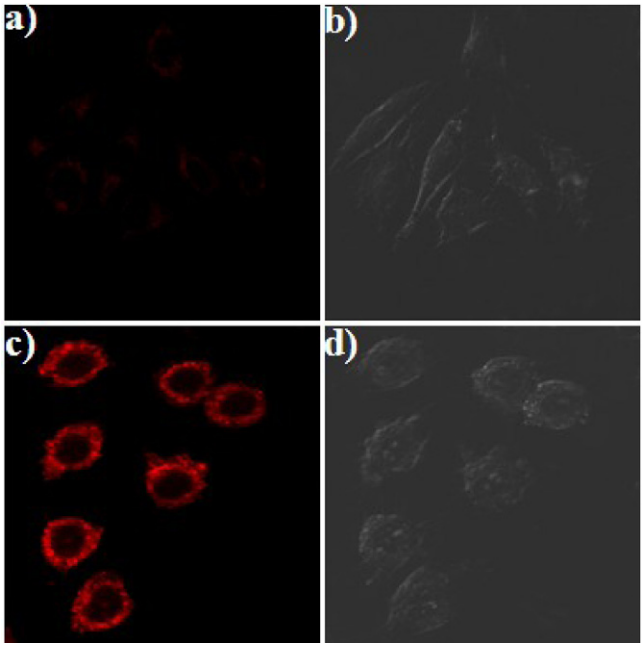

Fig. 6. Confocal fluorescence images in HeLa cells. (a) Cells incubated with 20 μM **NRC** in PBS buffer for 30 min; (b) brightfield image of cells shown in panel (a); (c) cells incubated with 1 μM Cu^{2+} for 30 min, washed three times, and then further incubated with 20 μM **NRC** for 30 min (ex = 559 nm); (d) brightfield image of cells shown in panel (c).

Table 1
Performances comparison of various fluorescent/colorimetric chemosensors for Cu^{2+} ion with signal enhancement.

Modes	Reagents	Reproducibility	Linear range (μM)	LOD (μM)	Testing media	Applications	Remarks	Ref.
Enhancement $\lambda_{ex/em}$ = 451/475–525 nm	Naphthalimide derivative	NA	0–0.1	0.01	Water–ethanol (6:4, v/v, pH 7.2, 50 mM HEPES)	NA	Fluorescent change, ratiometric chemosensor	[20]
Enhancement (UV–vis) λ_{abs} = 540 nm	Naphthalimide derivative	Reversible	0–5	0.3	Water–ethanol (8:2, v/v, pH 6.98, 10 mM Tris)	NA	Chromo-change	[21]
Enhancement $\lambda_{ex/em}$ = 360/430–481 nm	Naphthalimide derivative	NA	NA	NA	CH_3CN	NA	Fluorogenic change, ratiometric chemosensor	[22]
Enhancement $\lambda_{ex/em}$ = 370/450–544 nm	Naphthalimide derivative	NA	NA	NA	CH_3CN or HEPES–CH_3CN (1:1, v/v, pH 7.4, 500 mM HEPES)	NA	Dual chromo- and fluorogenic changes, ratiometric chemosensor	[16]
Enhancement $\lambda_{ex/em}$ = 510/580 nm	Rhodamine derivative	Reversible	0.05–0.9	0.003	Water–methanol (2:8, v/v, pH 7.0, 20 mM HEPES)	NA	Dual chromo- and fluorogenic changes	[17]
Enhancement $\lambda_{ex/em}$ = 540/586 nm	Rhodamine derivative	NA	0.001–0.01	NA	Water–CH_3CN (9:1, v/v, pH 7.0, 10 mM Tris–HCl)	NA	Dual chromo- and fluorogenic changes, dual-function chemosensor for Cu^{2+} and ClO^-	[18]
Enhancement $\lambda_{ex/em}$ = 495/552 nm	Rhodamine derivative	Reversible	NA	NA	Water–CH_3CN (1:1, v/v)	Ej cells	Dual chromo- and fluorogenic changes	[19]
Enhancement $\lambda_{ex/em}$ = 510/548 nm	Naphthalimide modified rhodamine 6G derivative	NA	0–10	NA	HEPES–CH_3CN (1:1, v/v, pH 7.4, 20 mM HEPES)	NA	Dual chromo- and fluorogenic changes, dual-function chemosensor for Cu^{2+} and Zn^{2+}.	[11]
Enhancement $\lambda_{ex/em}$ = 510/580 nm	Naphthalimide modified rhodamine derivative	Reversible	0.05–4.5	0.018	Water–ethanol (9:1, v/v, pH 7.0, 50 mM HEPES)	HeLa cells	Dual chromo- and fluorogenic changes	This work

NA: not available.

then treated with 20 μM **NRC** for 30 min. Moreover, brightfield measurements confirmed that the cells after treatment with Cu^{2+} and/or **NRC** were viable (Fig. 6(b and d)). These results revealed an excellent cell-membrane permeability of **NRC**. Furthermore, the chemosensor **NRC** was demonstrated applicable for in vitro imaging of Cu^{2+} in living cells and potentially in vivo.

3.6. Method performance comparison

The performance of the proposed chemosensor **NRC** toward Cu^{2+} was compared with some reported fluorescent/colorimetric chemosensors based on either naphthalimide or rhodamine B structural motif for Cu^{2+} determination, as shown in Table 1. All the methods present good selectivity for Cu^{2+} with signal enhancement, and most of them can adopt dual chromo- and fluorogenic changes toward Cu^{2+} [11,16–19], as well as our proposed **NRC**. A few of chemosensors possess wide quantitation span [11,17,18,21], or down to nM LOD [17,18], but some of them need more rigorous testing media and the applicability in living cells are not investigated. Notably, as for the two types of enhancement chemosensors based on rhodamine [18] and naphthalimide modified rhodamine derivatives [11], dual-function detection for Cu^{2+} and ClO^- [18], and dual-function detection for Cu^{2+} and Zn^{2+} [11] are realized, respectively, however, their applications in living cells are not validated, yet. Our newly developed chemosensor presents a number of attractive analytical features such as high sensitivity, wide linear range, good reproducibility, good selectivity and wide applicability. The fluorescent chemosensor **NRC** based on naphthalimide modified rhodamine spirolactame derivative is easy to prepare with low cost and can be used for rapid analysis of ultra-trace level Cu^{2+} in living cells.

4. Conclusions

In summary, a novel aqueous media-soluble fluorescent chemosensor **NRC** was presented for high sensitive determination of Cu^{2+} in both aqueous solutions and living cells. This sensing for Cu^{2+} could be attributed to the equilibrium between the spirolactam (non-fluorescence) and the ring-opened amide (fluorescence), a desirable "off-on" mode. The fluorescence intensity was linearily enhanced with Cu^{2+} concentration in starndard aqueous solution from 0.05–4.5 μM, with the detection limit of 0.018 μM. This indicated that the chemosensor could be applied for rapid monitoring and accurate quantification of trace Cu^{2+} in environmental water samples.

More importantly, the colorimetric and fluorescent chemosensor **NRC** attained remarkably specific discrimination of Cu^{2+} from other metal ions and anions, showing an excellent sensing system. Also, the living cell imaging suggested the chemosensor **NRC** was membrane-permeable and primarily non-toxic to cell culture, and therefore further demonstrated its great applicability for the high sensitive and selective determination of Cu^{2+} in living cells even in vivo.

Acknowledgements

This work was financially supported by the National Natural Science Foundation of China (20975089, 90913006, 21077068), the Innovation Projects of the Chinese Academy of Sciences (KZCX2-EW-206), the National Basic Research Program of China (2010CB933504), the Department of Science and Technology of Shandong Province (2008GG20005005), the Research and Training Foundation of Hainan Medical University (HY2010-004), and the 100 Talents Program of the Chinese Academy of Sciences.

Appendix A. Supplementary data

Supplementary data associated with this article can be found, in the online version, at doi:10.1016/j.talanta.2011.06.057.

References

[1] (a) A.P. de Silva, H.Q.N. Gunaratne, T. Gunnlaugsson, A.J.M. Huxley, C.P. McCoy, J.T. Rademacher, T.E. Rice, Chem. Rev. 97 (1997) 1515–1566;
(b) P. Jiang, Z. Guo, Coord. Chem. Rev. 248 (2004) 205–229;
(c) M.H. Lim, S. Lippard, J. Acc. Chem. Res. 40 (2007) 41–51.

[2] H. Tapiero, D.M. Townsend, K.D. Tew, Biomed. Pharmacother. 57 (2003) 386–398.

[3] R.A. Lovstad, BioMetals 17 (2004) 111–113.

[4] (a) P. Kaur, D. Sareen, K. Singh, Talanta 83 (2011) 1695–1700;
(b) Q. Wu, E.V. Anslyn, J. Am. Chem. Soc. 126 (2004) 14682–14683;
(c) L. Zeng, E.V. Mller, A. Pralle, E.Y. Isacoff, C.J. Chang, J. Am. Chem. Soc. 128 (2006) 10–11;
(d) N. Shao, Y. Zhang, S.M. Cheung, R.H. Yang, W.H. Chan, T. Mo, K.A. Li, F. Liu, Anal. Chem. 77 (2005) 7294–7303;
(e) G.X. Liang, H.Y. Liu, J.R. Zhang, J.J. Zhu, Talanta 80 (2010) 2172–2176;
(f) Y. Zheng, K.M. Gattás-Asfura, V. Konka, R.M. Leblanc, Chem. Commun. (2002) 2350–2351.

[5] (a) S. Goswami, R. Chakraborty, Tetrahedron Lett. 50 (2009) 2911–2914;
(b) H. Mu, R. Gong, Q. Ma, Y. Sun, E. Fu, Tetrahedron Lett. 48 (2007) 5525–5529.

[6] (a) Y. Zheng, J. Orbulescu, X. Ji, F.M. Andreopoulos, S.M. Pham, R.M. Leblanc, J. Am. Chem. Soc. 125 (2003) 2680–2686;
(b) Y. Xiang, A. Tong, Luminescence 23 (2008) 28–31;
(c) H.J. Kim, S.Y. Park, S. Yoon, J.S. Kim, Tetrahedron 64 (2008) 1294–1300;
(d) H.J. Kim, J. Hong, A. Hong, S. Ham, J.H. Lee, J.S. Kim, Org. Lett. 10 (2008) 1963–1966;
(e) W. Lin, L. Yuan, W. Tan, J. Feng, L. Long, Chem. Eur. J. 15 (2009) 1030–1035.

[7] (a) K. Rurack, M. Kollmannsberger, U. Resch-Genger, J. Daub, J. Am. Chem. Soc. 122 (2000) 968–969;
(b) J.S. Yang, C.S. Lin, C.Y. Hwang, Org. Lett. 3 (2001) 889–892;
(c) Y. Xiang, Z. Li, X. Chen, A. Tong, Talanta 74 (2008) 1148–1153;
(d) H. Yang, Z.Q. Liu, Z.G. Zhou, E.X. Shi, F.Y. Li, Y.K. Du, T. Yi, C.H. Huang, Tetrahedron Lett. 47 (2006) 2911–2914;
(e) W.C. Lin, C.Y. Wu, Z.H. Liu, C.Y. Lin, Y.P. Yen, Talanta 81 (2010) 1209–1215;
(f) Y. Zhao, X.B. Zhang, Z.X. Han, L. Qiao, C.Y. Li, L.X. Jian, G.L. Shen, R.Q. Yu, Anal. Chem. 81 (2009) 7022–7030.

[8] (a) E.M. Nolan, S.J. Lippard, Acc. Chem. Res. 42 (2009) 193–203;
(b) M. Fernandez-Suarez, A.Y. Ting, Nat. Rev. Mol. Cell Biol. 9 (2008) 929–943;
(c) O. Thoumine, H. Ewers, M. Heine, L. Groc, R. Frischknecht, G. Giannone, C. Poujol, P. Legros, B. Lounis, L. Cognet, D. Choquet, Chem. Rev. 108 (2008) 1565–1587;
(d) E.L. Que, D.W. Domaille, C.J. Chang, Chem. Rev. 108 (2008) 1517–1549.

[9] (a) J.F. Zhang, C.S. Lim, B.R. Cho, J.S. Kim, Talanta 83 (2010) 658–662;
(b) S.H. Yoon, E.W. Miller, Q.W. He, P.H. Do, C.J. Chang, Angew. Chem., Int. Ed. 46 (2007) 6658–6661;
(c) D.W. Domaille, E.L. Que, C.J. Chang, Nat. Chem. Bio. 4 (2008) 168–175;
(d) L. Xue, C. Liu, H. Jiang, Chem. Commun. (2009) 1061–1063;
(e) E.W. Miller, Q.W. He, C.J. Chang, Nat. Protoc. 3 (2008) 777–783;
(f) V.S. Shete, D.E. Benson, Biochemistry 48 (2009) 462–470;
(h) W.M. Liu, L.W. Xu, R.L. Sheng, P.F. Wang, H.P. Li, S.K. Wu, Org. Lett. 9 (2007) 3829–3832;
(i) T. Cheng, Y. Xu, S. Zhang, W. Zhu, X. Qian, L. Duan, J. Am. Chem. Soc. 130 (2008) 16160–16161.

[10] Y. Zhou, F. Wang, Y. Kim, S.J. Kim, J. Yoon, Org. Lett. 11 (2009) 4442–4445.

[11] J.F. Zhang, Y. Zhou, J. Yoon, Y. Kim, S.J. Kim, J.S. Kim, Org. Lett. 12 (2010) 3852–3855.

[12] (a) M. Beija, C.A.M. Afonso, J.M.G. Martinho, Chem. Soc. Rev. 38 (2009) 2410–2433;
(b) H.N. Kim, M.H. Lee, H.J. Kim, J.S. Kim, J. Yoon, Chem. Soc. Rev. 37 (2008) 1465–1472;
(c) R. Wang, C.W. Yu, F.B. Yu, L.X. Chen, Anal. Chem 29 (2010) 1004–1013.

[13] B. Liu, H. Tian, Chem. Commun. (2005) 3156–3158.

[14] X.F. Yang, X.Q. Guo, Y.B. Zhao, Talanta 57 (2002) 883–890.

[15] (a) M.I. Rodríguez-Cáceres, R.A. Agbaria, I.M. Warner, J. Fluoresc. 15 (2005) 185–190;
(b) H.A. Benesi, J.H. Hildebrand, J. Am. Chem. Soc. 71 (1949) 2703–2707.

[16] Z.C. Xu, J. Yoon, D.R. Spring, Chem. Commun. 46 (2010) 2563–2565.

[17] C.W. Yu, J. Zhang, R. Wang, L.X. Chen, Org. Biomol. Chem. 8 (2010) 5277–5279.

[18] Y.L. Liu, Y. Sun, J. Du, X. Lv, Y. Zhao, M.L. Chen, P. Wang, W. Guo, Org. Biomol. Chem. 9 (2011) 432–437.

[19] L. Huang, X. Wang, G.Q. Xie, P.X. Xi, Z.P. Li, M. Xu, Y.J. Wu, D.C. Bai, Z.Z. Zeng, Dalton Trans. 39 (2010) 7894–7896.

[20] Z.C. Xu, Y. Xiao, X.H. Qian, J.N. Cui, D.W. Cui, Org. Lett. 7 (2005) 889–892.

[21] J.H. Huang, Y.F. Xu, X.H. Qian, Dalton Trans. (2009) 1761–1766.

[22] Z.C. Xu, S.J. Han, C. Lee, J. Yoon, D.R. Spring, Chem. Commun. 46 (2010) 1679–1681.